Catalysis Letters (2018) 148:2373–2381
https://doi.org/10.1007/s10562-018-2448-7

# Highly Basic and Dipolar Layered Double Hydroxides Enhance Catalysis of Cyanoethylation of Alcohols

**Mariana Díaz[1] · Alejandra Santana Cruz[2] · Jorge Flores[2] · Ariel Guzmán[3] · Enrique Lima[1,2]**

Received: 22 March 2018 / Accepted: 6 June 2018 / Published online: 14 June 2018


## Abstract

Layered double hydroxides (LDH), magnesium–aluminum–carbonates and magnesium–gallium–aluminum–carbonates, were synthesized by sol–gel incorporating during synthesis a part of aluminum as $(AlF_6)^{3-}$ blocks in order to incorporate $F^-$ as a part of brucite-like layers and not as compensating anions. Structural, textural and surface properties of resulting fluorinated were characterized. Particularly, presence the fluorine as a part of brucite-like layers influenced directly polarity and hydrogen bonding acceptor character at surface of materials. These modifications at surface of LDH greatly changed their catalytic properties. Cyanoethylation reaction between acrylonitrile and methanol was catalyzed by both fluorine-free and fluorinated LDH, pointing out a clear influence of fluorine on the conversion and rate reaction.

## Graphical Abstract

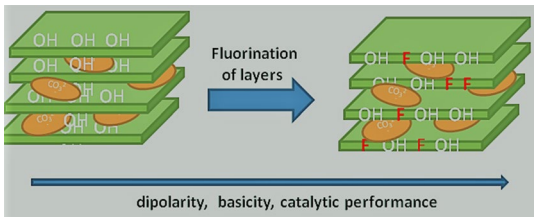


**Keywords** Layered double hydroxides · Catalysts · Basicity · Polarity · Cyanoethylation

## 1 Introduction

Acrylonitrile undergoes cyanoethylation with monohydric alcohols to give alcoxypropionitriles, which can be converted to different types of amines after hydrogenation or can form the related carboxylic acid through hydrolysis. Therefore, cyanoethylation is a commonly used reaction for the synthesis of drug intermediates and organic compounds of industrial interest [1].

This reaction is usually catalyzed by a base, which is typically a homogeneous basic catalyst such as alkali hydroxides or alkoxides [2] or tetraalkylammonium hydroxides [3]. However, the use of this kind of catalysts requires some extra steps before the purification of the product, generating waste, losing catalyst and reducing product yields.

Different materials have been proposed as heterogeneous catalysts for this reaction, which include anion

✉ Enrique Lima
lima@iim.unam.mx

[1] Laboratorio de Fisicoquímica y Reactividad de Superficies (LaFReS), Instituto de Investigaciones en Materiales, Universidad Nacional Autónoma de México, Circuito Exterior s/n, Cd. Universitaria, Del. Coyoacán, CP 04510, Mexico City, Mexico

[2] Universidad Autónoma Metropolitana, Azcapotzalco, Av. San Pablo 180, Col. Reynosa Tamaulipas, 02200 Mexico City, Mexico

[3] Instituto Politécnico Nacional - ESIQIE, Avenida IPN UPALM Edificio 7, Zacatenco, 07738 Mexico City, DF, Mexico

exchange resins [4, 5], alkaline earth oxides [6], cesium-modified zeolite Y [7]. Layered double hydroxides (LDHs), both activated [8, 9] as well as modified [10, 11], have also been evaluated.

LDHs can be understood from the structure of brucite ($Mg(OH)_2$) which is made up of linked octahedra of magnesium hydroxide sharing edges to form infinite layers. In LDHs, an isomorph substitution of $Mg^{2+}$ ion by a trivalent cation $M^{3+}$ has taken place. Due to the substitution, a positive charge is generated in the hydroxide layer which is compensated by a wide variety of anions in the interlayer region, along with water molecules, held through the formation of hydrogen bonds with the hydroxide layer OH and/or with the interlayer anions.

LDHs are described by the general formula $[M^{2+}_{1-x}M^{3+}_{x}(OH)_2][An^-]x/n{\cdot}mH_2O$, where $M^{2+}$ and $M^{3+}$ are the cations that occupy the octahedral positions within the hydroxide layer, $M^{2+}$ is typically $Mg^{2+}$ but may also be one of a number of divalent cations such as $Ni^{2+}$ or $Zn^{2+}$ [12]. In the same way, $M^{3+}$ may not only be $Al^{3+}$, but also $Cr^{3+}$, $Ga^{3+}$, $Fe^{3+}$, or another trivalent cation. x may vary between 0.17 and 0.33 for most of the couples of cations forming the sheet. $An^-$ represents the interlayer anion, which is normally carbonate, but larger anionic species are also known to occupy the space between the layers [13–15].

When LDHs are thermally treated, decomposition of anions, dehydroxylation of brucite-like layers and formation of mixed oxides occur.

Thus, mixed oxides obtained by thermal decomposition can promote base-catalyzed reactions such as aldol condensation [16, 17], hydrogenation [18–20], transesterification [21, 22] and steam reforming reactions [23].

If the calcination temperature is mild, between 200 and 400 °C, the obtained mixed oxides are able to recover the layered structure when put in contact with water or an anionic aqueous solution at low temperatures [24]. This property is called memory effect and has been employed for incorporating interlayer anions different from the original ones [25].

LDHs intercalated with $OH^-$ anions, known as meixnerite-type compounds or activated LDH, show Brönsted basic sites in catalytic reactions such as aldol condensation [26, 27], Claisen–Schmidt condensation [28], Knoevenagel reaction [26], and cyanoethylation of alcohols [8, 10, 11]. Activated LDHs are typically obtained through reconstruction in water of mixed oxides [25, 29].

The acid–base properties of LDH or of the resulting mixed oxides can be tuned by changing the nature of the cations forming the brucite-like layer [25] as well as the ratio $M^{2+}/M^{3+}$ [30], or selecting different species as compensating anions [29]. However, little has been done regarding the substitution of the OH structural groups.

In a recent paper, aluminum has been incorporated into the brucite-like sheets in the form of an octahedral aluminum fluorine complex during the synthesis [31]. The presence of fluoride anions modifies the textural, structural and thermal properties of the LDH. The replacement of structural $OH^-$ by $F^-$ in LDH has resulted in the enhancement of the hydrogen bond accepting (HBA) character and the acid–basicity of the material [32].

In this work, we have investigated the use of modified-fluorinated LDHs in the cyanoethylation of acrylonitrile with methanol, showing that fluoride content, rehydration time, as well as different trivalent cation content affect the conversion.

## 2 Experimental Procedures

### 2.1 Materials

Fluorine-free and fluorinated Mg/Al LDH with a Mg/Al atomic ratio close to 3 were prepared by sol–gel method reported elsewhere [33]. Aluminum tri-sec-butoxide (ATB) (Aldrich, 97%), sodium hexafluoroaluminate (SFA) and magnesium methoxide (MgM) (Aldrich, 10.16 wt% in methanol) were used as aluminum and magnesium sources. The hydrolysis catalyst used was $HNO_3$ (Baker, 70%); acetic acid (AA) (Baker, 99.8%) was employed to inhibit the polymerization reaction. Ethanol (Baker, 99%) was used as solvent. The synthesis procedure is as follows: ethanol was refluxed, and thereafter the aluminum tri-sec-butoxide was added and dissolved into the alcohol; the mixture was stirred for 1 h. Afterwards, a 3 N $HNO_3$ solution was added dropwise under vigorous stirring for 1 h, producing a transparent solution. The system was subsequently cooled to room temperature and AA was added under vigorous stirring for 1 h. In the following step, the system was cooled to 0 °C and MgM and SFA suspended in EtOH were slowly added. The solution was stirred at room temperature for 24 h and then deionized water was slowly added, allowing the hydrolysis to complete itself. The molar ratios of reactants were ATB:EtOH = 1:60, ATB:$HNO_3$ = 1:0.03, ATB:AA = 1:0.5, and ATB:$H_2O$ = 1:1. For the fluorine-free sample, ATB:MgM = 1:3. Appropriate amounts of ATB, SFA and MgM were used in order to maintain Mg/Al atomic ratio close to 3. The gel was poured into a glass vessel and was aged for 24 h at room temperature. The products were dried overnight at 80 °C.

Mg/Ga LDH with an atomic ratio close to 3 was prepared by coprecipitation method previously reported [34]. A 1 M aqueous solution containing appropriate amounts of ($Mg(NO_3)_2{\cdot}6H_2O$) (Aldrich 98%) and ($Ga(NO_3)_3{\cdot}xH_2O$) was delivered into a reactor by a peristaltic pump at a constant flow of 1 cm3/min. A second aqueous solution containing 1.0 M KOH (Aldrich, 99%) plus 0.075 M $K_2CO_3$ was

simultaneously fed. These two solutions were added dropwise into a flask containing 100 $cm^3$ of water at 40 °C upon vigorous stirring. The pH remained constant by controlling the addition of the alkaline solution using a pH-STAT Titrando apparatus (Metrohm, Switzerland). After completing the addition of the solutions, the white gel obtained was aged during 16 h at 80 °C and then washed several times. After this, the white paste was dried overnight at 80 °C.

For the fluorinated samples, SFA was used as fluorine source. These samples were obtained using a similar procedure as for the previous one, appropriate amount of SFA was suspended in the starting solutions containing ($Mg(NO_3)_2{\cdot}6H_2O$) and ($Ga(NO_3)_3{\cdot}xH_2O$). Table 1 summarizes the samples under study in this work.

## 2.2 Characterization

The samples were characterized by X-ray diffraction (XRD), nuclear magnetic resonance (MAS NMR) of $^{27}Al$ and $^{19}F$ nuclei, and $N_2$ adsorption. The XRD patterns were acquired using a diffractometer D8 Advance-Bruker equipped with a copper anode X-ray tube. The presence of pure LDH (native sample) and periclase (sample thermally activated) structures was confirmed by fitting the diffraction patterns with the corresponding Joint Committee Powder Diffraction Standards (JCPDS cards). The single pulse solid-state $^{27}Al$ and $^{19}F$ MAS NMR single excitation spectra were acquired on a Bruker Avance 300 spectrometer. The single pulse $^{27}Al$ NMR spectra were acquired under MAS conditions by using a Bruker MAS probe with a cylindrical 4 mm o.d. zirconia rotor and by operating the spectrometer at a frequency of 78.1 MHz. Short single pulses (π/12) were used. The 90° solid pulse width was 2 μs, and the chemical shifts were referenced to those of an aqueous 1 M $AlCl_3$ solution. The MAS frequency was 10 kHz. All the NMR measurements were done at room temperature (19 °C). The $^{19}F$ MAS NMR spectra were measured by operating the spectrometer at 376.3 MHz, using π/2 pulses of 6 ms with a recycle delay of 1 s; $^{19}F$ chemical shifts were referenced to those of $CFCl_3$ at 0 ppm.

The nitrogen adsorption–desorption isotherms were determined with Bel-Japan Minisorp II equipment, using a multipoint technique. Surface areas were calculated with the BET equation.

Three dyes were adsorbed with the purpose to evaluate the polarity parameters of LDH. Dicyano-bis-(1,10-phenanthroline)-iron(II) complex; 3-(4-amino-3-methylphenyl)-7-phenyl-benzo-[1,2-b:4,5-b0]-difuran-2,6-dione and 4-tert-butyl-2-(dicyanomethylene)-5-[4-(diethylamino) benzylidene]-Δ-thiazoline. Adsorption of dyes was done according to the procedure followed earlier [35]. Briefly, first dye was dissolved in dichloromethane and last two dyes were dissolved in cyclohexane. After that 0.1 g of the LDH were suspended in 5 ml of dye solution and shaken for 15 min keeping out of light; the colored HDL was recovered and dried under vacuum. The shifts UV/vis absorption band of the probe dyes resulting from both rather specific [hydrogen bond donating (HBD) and HBA] and non-specific interactions (dipole–dipole, dipole–induced dipole, or London dispersion forces). The evaluation of the polarity of samples was determined applying the multi-parameter approach of Kamlet–Taft [36–38]. The simplified Kamlet–Taft equation is the following: $\nu_{max} = \nu_{max,0} + a\alpha + b\beta + s\pi$; where $\nu_{max,0}$ denotes the peak frequency value of a solvent reference system. The parameter α describes the HBD ability, β the HBA ability, and π* represents the dipolarity/polarisability. Further, a, b, and s are solvent-independent coefficients reflecting contributions of solvent effects to the UV/vis absorption shift νmax. α, β, and π* can be individually derived [36] from the UV/vis absorption maxima of the three perichromic probe dyes selected.

## 2.3 Cyanoethylation Catalytic Tests

The catalyst activation was performed in a two-step process: Typically, 0.1 g of the as-synthesized LDH was heat-treated with a heating rate of 5 °C/min, up to 400 °C, where it was maintained for 6 h. Thereafter, the sample was rehydrated with decarbonated water, for 24 h at room temperature.

**Table 1** Chemical composition and specific surface area of LDH samples

| Sample code | F percent (wt%) | Chemical formula | Specific surface area[a] ($m^2/g$) |
|---|---|---|---|
| MA | 0.00 | $[Mg_{0.775}Al_{0.253}(OH)_2](CO_3)_{0.127}{\cdot}0.51H_2O$ | 10.26 |
| MAF10 | 2.99 | $[Mg_{0.743}Al_{0.248}(OH)_{1.88}F_{0.12}](CO_3)_{0.124}{\cdot}0.52H_2O$ | 11.67 |
| MAF20 | 8.68 | $[Mg_{0.739}Al_{0.239}(OH)_{1.65}F_{0.35}](CO_3)_{0.119}{\cdot}0.55H_2O$ | 74.94 |
| MG | 0.00 | $[Mg_{0.769}Ga_{0.250}(OH)_2](CO_3)_{0.125}{\cdot}0.51H_2O$ | 51.75 |
| MGF10 | 1.94 | $[Mg_{0.777}Ga_{0.229}Al_{0.023}(OH)_{1.91}F_{0.09}](CO_3)_{0.126}{\cdot}0.60H_2O$ | 87.48 |
| MGF20 | 8.36 | $[Mg_{0.773}Ga_{0.168}Al_{0.094}(OH)_{1.62}F_{0.38}](CO_3)_{0.131}{\cdot}0.57H_2O$ | 89.71 |

[a]As determined from $N_2$ isotherms applying the BET method. Previous to $N_2$ adsorption analysis the samples were treated under vacuum only at 70 °C assuring they preserve the layered structure

The cyanoethylation reaction procedure was similar to that previously reported [8]. Typically, 40 mmol of acrylonitrile and 10 mL of methanol were added to a three-necked 25-mL round-bottom flask equipped with a reflux condenser and a thermometer. The solution was magnetically stirred at 50 °C, and the freshly activated catalyst was rapidly added to the reactor in order to minimize exposure to atmospheric $CO_2$. Once the reaction started, aliquots were periodically taken from the reaction mixture, filtered and analyzed on a QP2010SE GC–MS equipped with a 30 m Rtxi-5 ms (5%-phenyl-methylpolysiloxane) capillary column. Conversion was calculated following the decrease in acrylonitrile concentration.

## 3 Results and Discussion

### 3.1 Catalysts

XRD patterns of LDH samples are shown in Fig. 1. Firstly, it have to be mentioned that all activated catalysts maintain the hydrotalcite phase, i.e. they are layered materials. Any significant changes are observed in XRD patterns as a consequence of the fluorine content. In magnesium–aluminum series, the peaks are broad as often observed for samples synthesized by a sol–gel method; the peak indexed 003 was observed at 11.3° consistent with an interlayer spacing of 23.27 Å. The samples containing gallium exhibited narrow peaks as they were synthesized by co-precipitation method. The position of peak 003 estimates an interlayer distance of 23.46 Å for these samples. None fluorine compound was detected in both samples series.

The $^{27}$Al MAS NMR spectra of activated catalysts are included in Fig. 2 Independently of the presence or the

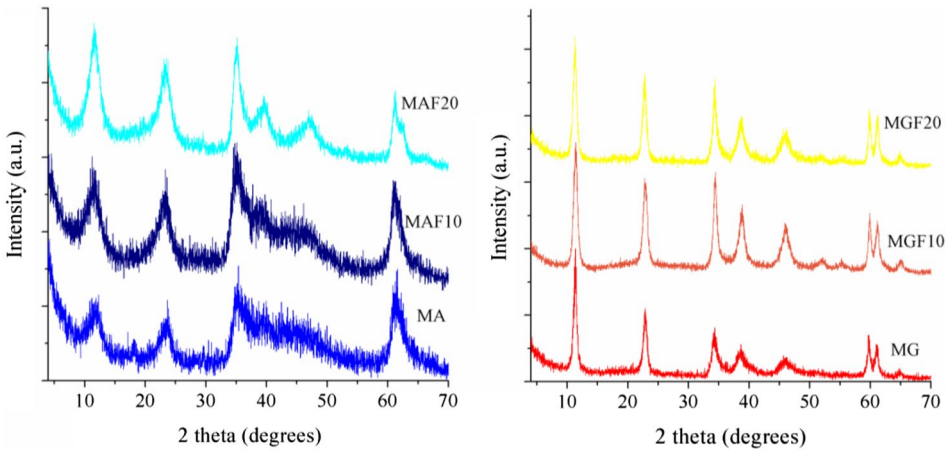


**Fig. 1** XRD patterns of LDH containing fluorine as a part of brucite-like layers. Samples Mg–Al (left) and samples Mg–Ga (right)

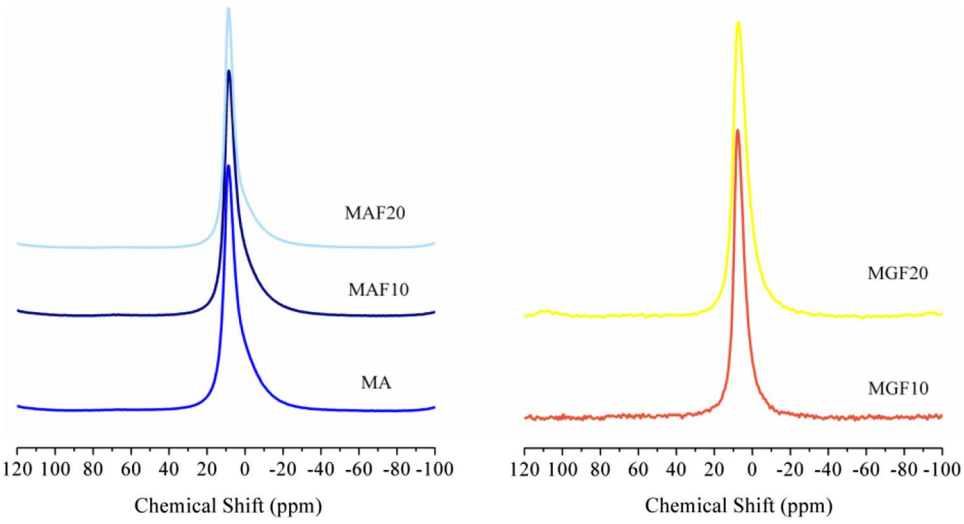


**Fig. 2** $^{27}$Al NMR MAS spectra of LDH containing fluorine as a part of brucite-like layers. Samples Mg–Al (left) and samples Mg–Ga (right)

absence of fluorine, the spectra are composed by a single isotropic peak close to 0 ppm, confirming the sixfold coordination of aluminum in all catalysts [39]. However, in spectra of magnesium–aluminum samples, the peak broadness increases slightly with the presence of fluorine suggesting a spread in chemical shift which is in line with the first neighbored atoms of aluminum being only oxygen for sample MA and being oxygen and fluorine for samples MAF. In spectra of samples magnesium–aluminum–galium, the NMR peak became broader with the presence of fluorine. Here the aluminum atoms modify their first neighbors when fluorine is present but also the second neighbors are heterogeneous as they could be Mg or Ga.

$^{19}$F MAS NMR spectra of LDH samples are shown in Fig. 3, where one can see that, regardless the amount of fluorine that was introduced into LDH, two NMR peaks for fluorine-containing LDHs are observed in spectra samples MAF. The first peak at − 173.1 ppm is assigned to $AlF_{6-x}O_x$ species enriched in oxygen and the second one centered at − 164 ppm suggest that $AlF_{6-x}O_x$ species tends to balance the number of oxygen and fluorine atoms in the aluminum octahedral [40]. Actually, the most intense peak is that of − 164 ppm, which is in line with previous work [31] showing that a cycle calcination-rehydration induces a homogeneous repartition of fluorine into brucite-like layers. In spectra of samples MGF both peaks mentioned above are observed but also a third peak at low field (− 156 ppm) is also observed. The NMR peak due to $(GaF_6)^{3-}$ species is reported around − 140 ppm [41]. Thus, the peak at − 156 ppm should be assigned to species $GaF_{6-x}O_x$, which are formed because of introduction of blocks $(AlF_6)^{3-}$ instead $(Ga(OH)_6)^{3-}$. Even when the fluorine is added as a part of $(AlF_6)^{3-}$, the insertion of these block in brucite-like layer assures that second neighbor of fluorine is either $Mg^{2+}$ or $Ga^{2+}$.

From structural characterization above described about fluorination of LDHs is clear that insertion of fluorinated blocks is possible in Mg–Al and Mg–Ga LDHs, it remains open the question if this structural modification is enough to modify significantly the surface of LDH and subsequently their catalytic properties. In this sense, the Fig. 4 displays representative UV/vis absorption spectra of dye dicyano-bis-(1,10-phenanthroline)-iron(II) complex adsorbed on the

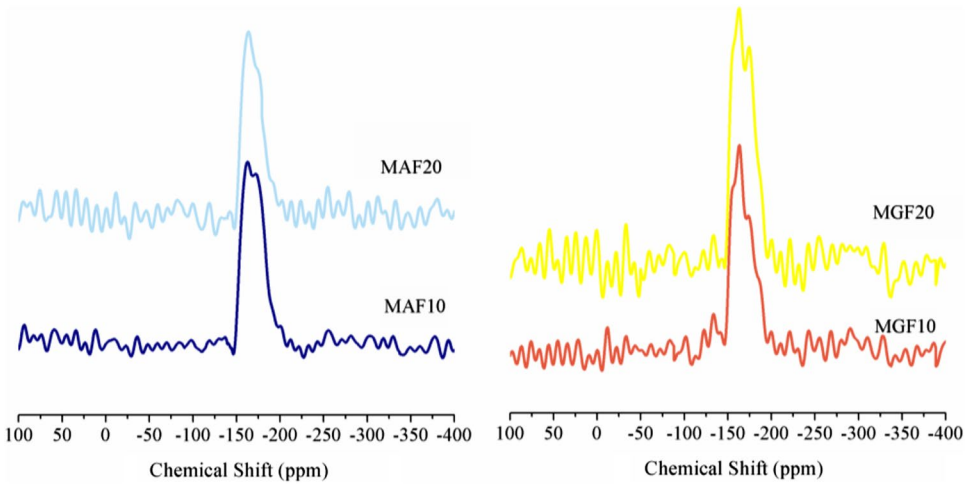


**Fig. 3** $^{19}$F NMR MAS spectra of LDH containing fluorine as a part of brucite-like layers. Samples Mg–Al (left) and samples Mg–Ga (right)

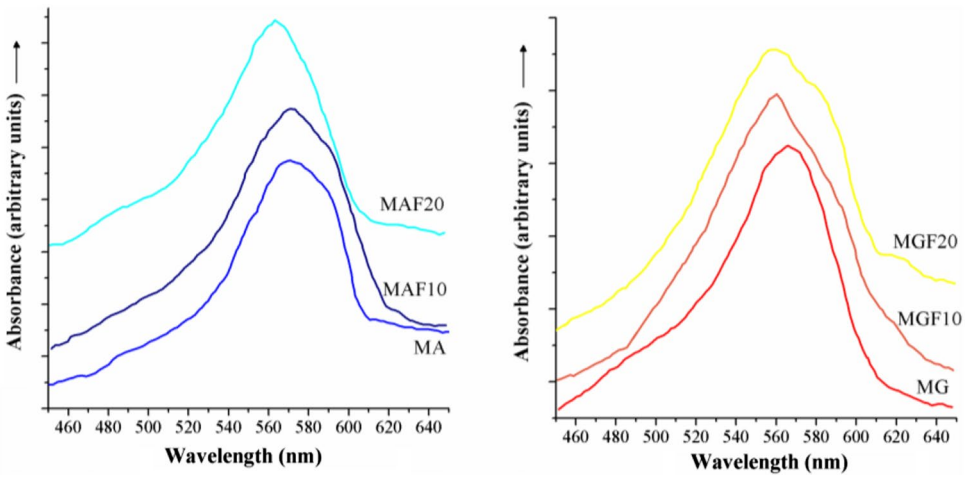


**Fig. 4** UV–vis spectra of the indicator dye $Fe(phen)_2(CN)_2$ adsorbed onto fluorinated LDH Mg–Al (left) and fluorinated LDH Mg–Ga (right)

LDHs. As earlier reported, the UV/vis absorption band can be fitted with two Gaussian components. The position of component at higher wave-length varied with the content of fluorine, a bathochromic effect was observed: position of this component was observed at 550 nm on MA sample but it is red shifted to 561, and 566 on the sample MAF and samples, respectively. The second component at lower wavelength was identified with an unaffected position at 583 ± 4 nm for all spectra. Bathochromic effects are definitely related to perturbing the distribution of pi electrons as a consequence of the interactions dye-LDH surface. With the UV–vis absorption maxima values of the components, the Kamlet–Taft surface polarity parameters (α, β, π*) of the LDHs surfaces were determined by applying the established method [36–38]. Values of α, β and π* for the various LDH are reported in Table 2.

The value of α is proportional to the hydrogen bonding donor (HBD) character of the surface. From Table 2, the LDH surfaces do not vary considerably their HBD character which is explained because replacement of $OH^-$ by $F^-$ is structural and apparently the amount of fluorine is not enough to impact significantly in the population of $OH^-$ at surface of LDH, in other words, OH at surface are likewise accessible to form hydrogen bonds when sample is fluorinated or free-fluorine.

A more interesting evolution was observed for the β and π* parameters. β parameter value is proportional to the hydrogen bonding acceptor (HBA) character. In Mg–Al series, β increases with the content of fluoride which is not surprising because of the ability of F to form strong hydrogen bonds. The higher values of β in fluorinated LDHs than those in free-fluorine samples suggest that both F and O are available at LDH surface to accept hydrogens, in other words, basic centers at surface of LDH increases with fluorination. Surprising, β increases in Mg–Ga when a low amount of fluorine is present but at high amount of fluorine a slightly decreases in β value is observed. Note that gallium and aluminum coordinate similarly to fluorine and oxygen, which is in line with the six-fold coordination of aluminum as evidenced by NMR. However, it seems that at high amount of fluorine, oxygen atoms in groups Ga–O–H have a higher HBD character than fluorine in Ga–F.

**Table 2** Kamlet–Taft's α, β, and π* values of LDH surfaces

| Sample code | α | β | π* |
|---|---|---|---|
| MA | 0.66 | 0.21 | 0.81 |
| MAF10 | 0.68 | 0.25 | 0.88 |
| MAF20 | 0.71 | 0.30 | 0.94 |
| MG | 0.65 | 0.23 | 0.80 |
| MGF10 | 0.70 | 0.31 | 0.92 |
| MGF20 | 0.73 | 0.26 | 1.01 |

The polarity parameter, π*, characterizes the dipolarity/polarizability character of the surface. This parameter increases significantly with the content of fluorine, which was expected as the chemical composition of surface changes creating different dipole moments at LDH surface. As previously reported, OH groups could be attracted by F stronger than by O creating thus a different orientation of dipole moments. This time, the dipolarity/polarizability character differs between Mg–Al and Mg–Ga series. With the fluorine content, in Mg–Ga samples the π* parameter augments more than in Mg–Al samples. Even when Ga and Al have similar electronegativities, they differ in size, thus, gallium being bigger influences the polarizability character at LDH surface.

The characterization described above supports that LDH series includes materials different between them and their surfaces are subtle varied regarding HBA, HBD and dipolarity/polarizability character as a consequence of the introduction of fluorine into the brucite-like layers.

From Table 1 is also pointed out that the presence of fluorine improves the specific surface area. However no direct correlation was found between the surface area and the Kamlet–Taft's α, β, and π* parameters. Now, are these changes enough to significantly modify their catalytic properties? The answer to this question is included in next section.

## 3.2 Catalysis

Preliminary catalytic tests (results not showed) pointed out that the conversion in cyanoethylation is really poor when the catalysts are used as synthesized or thermal treated. Then, the following results are that obtained with the catalysts activated as above described (thermal treated-rehydrated).

In Fig. 5 is plotted the conversion achieved with rehydrated Mg–Al catalysts. It can be seen that the initial conversion reached with free-fluorine catalyst is very poor (6%) and similar than that of fluorinated catalysts containing a low amount of fluorine; In contrast, MAF20 solid is always the most active solid achieving 22% of conversion after 30 min that reaction was started. For reaction times longer than 30 min, this catalyst increases significantly its activity reaching a conversion close to 80% after 3 h of reaction. The free-fluorine LDH is always the lowest efficient catalyst leading to a 23% conversion after 3 h of reaction.

The conversion values achieved after 3 h of reaction are plotted in Fig. 6. The catalysts containing gallium were clearly more active than that of Mg–Al series. The maximal conversion obtained using the rehydrated MG catalyst without fluorine is 97.4%. The fluorinated Mg–Ga catalysts behave differently than the fluorinated Mg–Al. The catalyst Mg–Ga with the lowest amount of fluorine is the most active leading to a conversion of 100% and a decrease in conversion to 84% was observed with the catalyst containing the

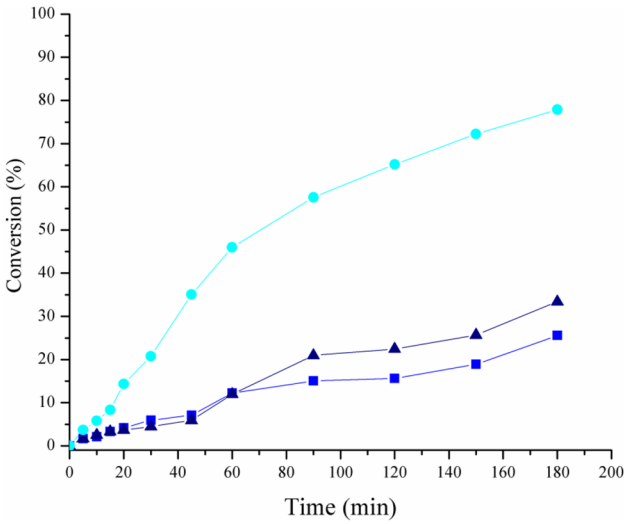


**Fig. 5** Conversion vs. time-on-stream data for the cyanoethylation between acrylonitrile and methanol over the calcined-rehydrated Mg–Al LDH

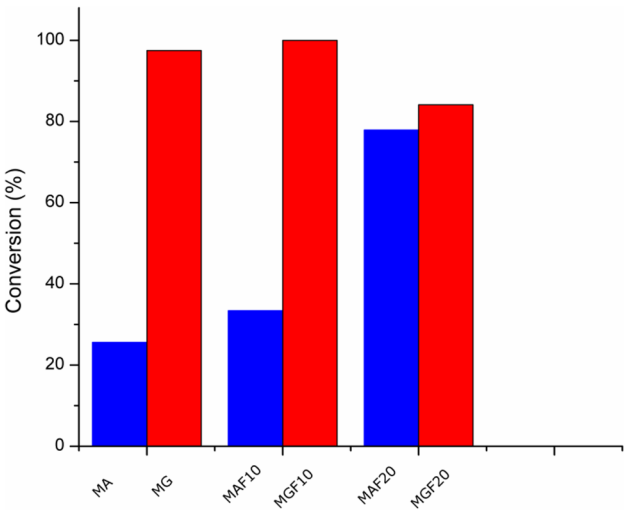


**Fig. 6** Maximal conversion achieved for the cyanoethylation between acrylonitrile and methanol as a function of the fluorine content in LDH catalysts

highest amount of fluorine. The surprising trend observed for catalysts Mg–Ga can be explained by character HBD and polarity/polarizability of samples. On the one hand, activation of multiple bond is favored by the increase of dipolarity induced with fluorine. On the other hand, a high amount of fluorine leads to a decrease in HBD character, in other words the ability of surface to attract protons and form anions, which is an important step in cyanoethylation mechanism, is reduced.

Table 3 includes the initial rate of reaction obtained with both catalyst series. In line with the conversion data

**Table 3** Initial rate of reaction of cyanoethylation using LDH catalysts

| Catalysts | Initial rate (mol $g_{cat}^{-1} min^{-1}$) |
|---|---|
| MA | $3.503 \times 10^{-4}$ |
| MAF10 | $4.084 \times 10^{-4}$ |
| MAF20 | $2.083 \times 10^{-3}$ |
| MG | $6.181 \times 10^{-3}$ |
| MGF10 | $9.855 \times 10^{-3}$ |
| MGF20 | $7.321 \times 10^{-3}$ |

previously discussed, the initial rate reached with Mg–Al are always slower than those obtained for the catalyst Mg–Ga. Catalysts MA and MAF10 leads to similar initial rates but the reaction proceeds 10 times faster with the catalyst containing highest amount of fluorine (MAF20). In series Mg–Ga the lowest rate is obtained also with the free-fluorine sample (MG). A high amount of fluorine in this sample series, catalyst MGF20, induces only a slightly increase in the initial rate. In contrast, the catalyst with a moderate amount of fluorine, catalyst MGF10, leads to the fastest rate among not only in this catalyst series but in all catalyst tested.

In Fig. 7 is plotted the conversion and initial rate of reaction as a function of two parameters of catalysts, the dipolarity/polarizability (parameter π*) and HBD character (parameter β). None simple function is evident but definitely is demonstrated that final conversion is influenced importantly by two parameters, two zones are easily identified, low conversions with the lowest values of two parameters and high conversions are achieved when both parameters increases. The influence of these parameters is less clear on the initial rate of reaction, points are well distributed in graph and the best catalyst is that with a moderate dipolarity/polarizability and HBD revealing that high values of these parameters do not necessarily play a positive role for this reaction. This result should be understood as the progress of the reaction needs a balance of the production of anions (necessities of moderate HBD) and activation of multiple bonds (needs of moderate π*). Actually, as mentioned above, the specific surface area also varied with the amount of fluorine in LDH. In this sense, the conversion as a function of HBD/specific surface area and π*/specific surface ratios clearly classify the catalysts in two groups: the first containing LDH with low values for π*, HBD and specific surface area which are low efficient catalyst (low conversion). The second group represents the catalysts more efficient and contain the LDHs with the highest values of specific surface area, π* and HBD. In other reactions the benefic role of number and strength of basic sites in LDH has been evidenced, for instance in transesterification of glycerol with dimethyl carbonate [42].

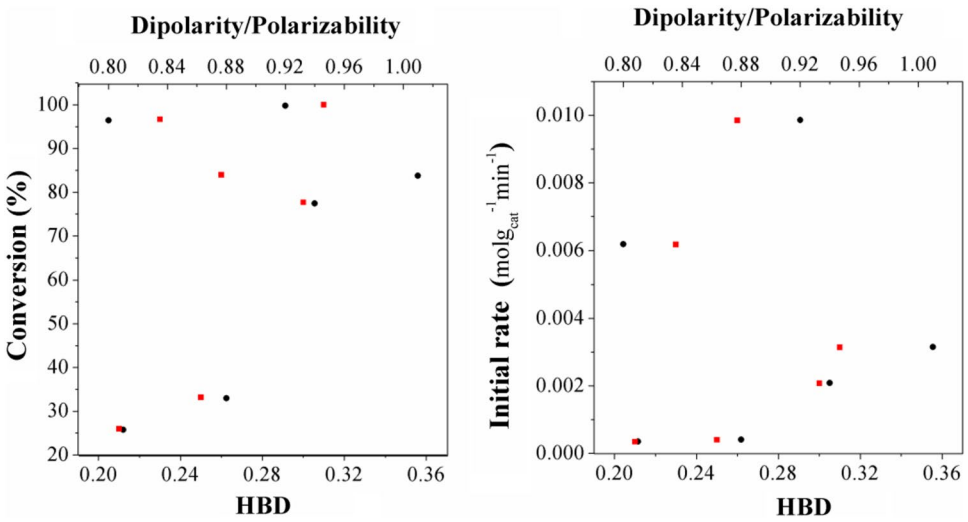


**Fig. 7** Conversion and rate reaction as a function of polarity parameters of catalysts

## 4 Conclusion

The replacement of structural $OH^-$ by $F^-$ in brucite-like layers induce changes in HBD (parameter β) character as well as in dipolarity/polarizability (parameter π*) whereas the HBA character is practically unchanged. If $F^-$ is introduced as a part of layers of Mg–Al LDHs the parameter β and π* increases up to 66 and 16%, respectively. In contrast, if $F^-$ replaces $OH^-$ in layers of Mg–Ga LDHs β increases only 35% and π* augments up to 25%. These modified LDHs can be more or less active catalysts in cyanoethylation reaction between acrylonitrile and methanol. Catalysts with low β and π* values lead to a low conversion and slow initial rates of reaction. With increase of β and π* both initial rate and conversion are improved. However, the catalyst with the highest value of π* and a high value of β is not the best catalyst. Actually, the 100% of conversion and the fastest rate are achieved with the catalyst presenting the highest β value and one of the highest π*. The dipolarity/polarizability is a very important surface parameter for reaction proceeds but a crucial parameter is the HBD or base character.

**Acknowledgements** This work was financially supported by CONACYT (Grant 220436) and PAPIIT-IN106517. We are also grateful to G. Cedillo and A. Tejeda for their technical assistance.

## References

1. Bruson HA (1949) Organic reactions V. In: Adams R (ed) Organic reactions V. Wiley, New York, pp 79–135
2. MacGregor JH, Pugh C (1945) J Chem Soc 535
3. Utermohlen WP (1945) J Am Chem Soc 67:1505
4. Astle MJ, Etherington RW (1952) Ind Eng Chem 44:2871
5. Trinadh M, Rajasekhar T, Bhadru B, Gopinath J, Santosh V, Reddy BVS, Sainath AVS (2013) J Appl Polym Sci 128:795
6. Kabashima H, Hattori H (1998) Catal Today 44:277
7. Zamanian S, Kharat AN (2014) Chin J Catal 35:264
8. Kumbhar PS, Sanchez-Valente J, Figueras F (1998) Chem Commun 10:1091
9. Valente J, Pfeiffer H, Lima E, Prince J, Flores J (2011) J Catal 279:196
10. Angelescu E, Pavel OD, Che M, Bîrjega R, Constentin G (2004) Catal Commun 10:647
11. Bîrjega R, Pavel OD, Costentin G, Che M, Angelescu E (2005) Appl Catal A 288:185
12. Miyata S (1975) Clays Clay Miner 23:369
13. Miyata S (1983) Clays Clay Miner 31:305
14. Ulibarri MA, Hernandez MJ, Cornejo J (1991) J Mater Sci 26:1512
15. Braterman PS, Ping Xu Z, Yarberry F (2004) Layered double hydroxides. In: Auerbach SM, Carrado KA, Dutta PK (eds) Handbook of layered materials. CRC Press, New York, pp 373–474
16. Choudary BM, Kantam ML, Kavita B, Reddy CV, Rao K, Figueras F (1998) Tetrahedron Lett 39:3555
17. Hora L, Kelbichová V, Kikhtyanin O, Bortnovskiy O, Kubička D (2014) Catal Today 138
18. Monzón A, Romeo E, Royo C, Trujillano R, Labajos FM, Rives V (1999) Appl Catal A 185:53
19. Coq B, Tichit D, Ribet S (2000) J Catal 189:117
20. Barrault J, Derouault A, Courtois G, Maissant JM, Dupin JC, Guimon C, Martinez H, Dumitriu E (2004) Appl Catal A 262:43
21. Liu Y, Lotero E, Goodwin JG Jr, Mo X (2007) Appl Catal A 138
22. Li E, Zhi PX, Rudolph V. Appl Catal B (2009) 88:42
23. Turco M, Bagnasco G, Costantino U, Marmottini F, Montanari T, Ramis G, Busca G (2004) J Catal 228:43
24. Cavani F, Trifirò F, Vaccari A (1991) Catal Today 11:173
25. Prinetto F, Ghiotti G, Robert D, Tichit D (2000) J Phys Chem B 104:11117
26. Lakshmi Kantam MB, Choudary M, Reddy CV, Koteswara Rao K, Lakshmi Kantam M, Choudary BM, Koteswara Rao K, Figueras F (1998) Chem Commun 32:1033
27. Roelofs JCAA., Lensveld DJ, Van Dillen AJ, De Jong KP (2001) J Catal 203:184
28. Climent MJ, Corma A, Iborra S, Velty A (2004) J Catal 221:474
29. Constantino VRL, Pinnavaia TJ (1995) Inorg Chem 34:883
30. Prescott HA, Li ZJ, Kemnitz E, Trunschke A, Deutsch J, Lieske H, Auroux A (2005) J Catal 234:119
31. Lima E, Martínez-Ortiz MJ, Gutiérrez Reyes RI, Vera M (2012) Inorg Chem 51:7774
32. Lima E, Pfeiffer H, Flores J (2014) Appl Clay Sci 88–89:26

33. Valente JS, Cantú M, Cortez JGH, Montiel R, Bokhimi X, López-Salinas E (2007) J Phys Chem C 111:642
34. López-Salinas E, Garcia-Sánchez M, Ramón-Garcia ML, Schifter I (1996) J Porous Mater 3:169
35. Lungwitz R, Spange S (2008) New J Chem 32:392
36. Spange S, Prause S, Vilsmeier E, Thiel WR (2005) J Phys Chem B 109:7280
37. Spange S, Zimmermann Y, Graeser A (1999) Chem Mater 11:3245
38. Spange S, Schmidt C, Kricheldorf HR (2001) Langmuir 17:856
39. Lippmaa E, Samoson A, Mägi M (1986) J Am Chem Soc 108:1730
40. Scholz G, Stosiek C, Noack J, Kemnitz E (2011) J Fluorine Chem 132:1079
41. Krahl T, Ahrens M, Scholz G, Heidemann D, Kemnitz E (2008) Inorg Chem 47:663
42. Zhang W, Wang D. Ma J, Wei W (2017) Catal Lett 147:1181